Sensors & Actuators: B. Chemical 349 (2021) 130794

Contents lists available at ScienceDirect

Sensors and Actuators: B. Chemical

journal homepage: www.elsevier.com/locate/snb

Wearable breath monitoring based on a flexible fiber-optic humidity sensor

Weijia Bao [a,b], Fengyi Chen [c], Huailei Lai [a,b], Shen Liu [a,b,*], Yiping Wang [a,b]

[a] Shenzhen Key Laboratory of Photonic Devices and Sensing Systems for Internet of Things, College of Physics and Optoelectronic Engineering, Shenzhen University, Shenzhen 518060, China
[b] Guangdong and Hong Kong Joint Research Centre for Optical Fibre Sensors, Shenzhen University, Shenzhen 518060, China
[c] School of Physics, Northwest University, Shaanxi 710069, China

ARTICLE INFO

Keywords:
Fiber Bragg grating
Fiber sensor
Wearable device
Breath sensor

ABSTRACT

Breath, as an important health monitoring indicator, provides valuable diagnostic information for cardiovascular disease and pulmonary function. Humidity can act as a bridge between breath and sensing signals. Current monitoring methods depend on humidity-sensitive material characteristics. In this work, an all fiber-optic flexible humidity sensor for wearable breath monitoring is reported. An eccentric fiber Bragg grating (EFBG) is inscribed in a single mode fiber to excite a stable core mode and sensitive cladding modes. The core mode is shown to maintain stable spectral features under a high-humidity atmosphere and can be used to calibrate the wavelength and power of the system. Importantly, the interface evanescent field of the cladding mode is highly sensitive to the ambient refractive index (RI) and even humidity-induced RI variation. Without combining any sensitized material, EFBG can directly perceive humidity fluctuations during breath with fast response (92 ms) and recovery times (100 ms). Different breathing patterns can be recognized, and breathing frequency can be extracted by sensor responses. The EFBG humidity sensor demonstrates great reproducibility, fast response, high flexibility, excellent robustness, and self-compensation capability, showing promising potential for wearable breath monitoring.

1. Introduction

Breath is a critical index used for body health monitoring and disease diagnosis [1–3]. Abnormal breath frequency and tidal volume might be symptoms of cardiovascular disease [4,5], neuropsychiatric disorders [6], sleep apnea syndrome [7,8], and the notorious coronavirus disease 2019 (COVID-19) [9]. Breath monitoring is necessary for prognostic judgment and illness observation.

Classic breath monitoring is mostly indirect. Humans will complete the expansion and constriction of the chest and exhale heat through their nose while breathing. Pressure sensors [10,11] and thermal sensors [12,13] can be used to monitor these two processes and then reveal breath states. The fixation methods of sensors or environmental temperature fluctuations have negative effects on monitoring results. Their comfort, operability and dimensions are not suitable for sick patients. Alternatively, humidity is a relatively direct parameter that can be used to characterize human breathing because the airflow relative humidity (RH) exhaled by humans can sharply reach over an RH of 90% from the room RH range (30–60%) [14]. This RH rise will not be influenced by the environment, weather or even movements. Therefore, a convenient and fast-response humidity sensor is highly desired for breath monitoring.

Humidity-sensitive material-based sensors have been extensively utilized for breath monitoring in recent years. The sorption and desorption rate of water molecules (i.e., humidity) dominate responses to human breathing, ranging from subseconds to minutes. A single breathing period is approximately 3–5 s and could sometimes be less than 1 s. Therefore, humidity sensors used for breath monitoring demand fast response and recovery times, and slow-response humidity-sensitive materials are not available. Graphene materials [15–17] supramolecular materials [18], nanowires [19–23], leather [24] and hydrophilic polymers [25–28] are great candidates for fast-response humidity-sensitive materials. These materials can be combined with flexible substrates, such as silicon chips [16,18,29,30], optical fibers [17,25,31–34] and plastic [23]. However, both graphene materials and organic materials suffer from tough film transfer processes and poor processability. Nanowires require a particular and costly growth technique, which is unsuitable for batch preparation. Polymer materials

* Corresponding author at: Shenzhen Key Laboratory of Photonic Devices and Sensing Systems for Internet of Things, College of Physics and Optoelectronic Engineering, Shenzhen University, Shenzhen 518060, China.
E-mail address: shenliu@szu.edu.cn (S. Liu).

https://doi.org/10.1016/j.snb.2021.130794
Received 20 May 2021; Received in revised form 29 July 2021; Accepted 19 September 2021
Available online 25 September 2021

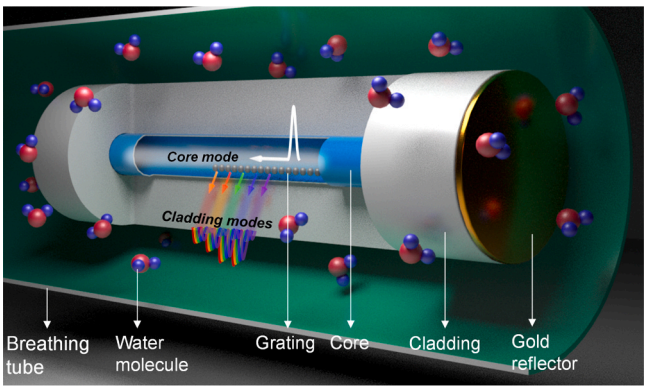

Fig. 1. Schematic configuration of the EFBG.

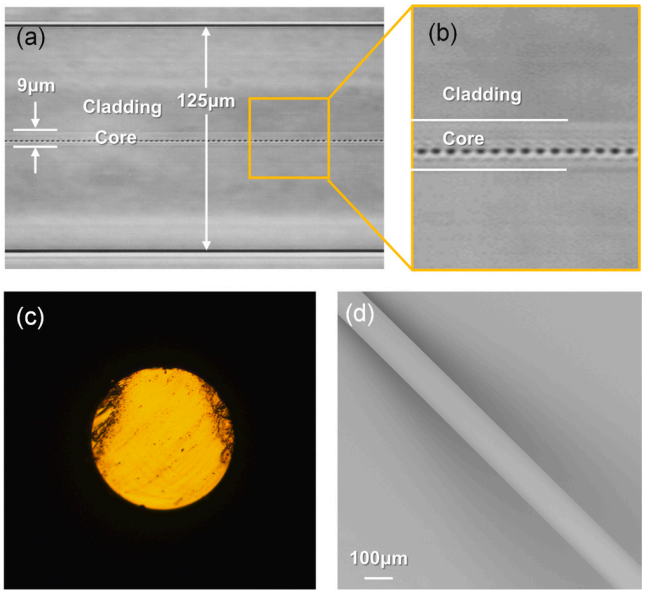

Fig. 2. (a) Side-view microscope of the EFBG; (b) enlarged microscope of the EFBG; (c) gold film covered on the fiber end; (d) scanning electron microscope (SEM) image of the fiber lateral surface.

have very good processing properties, such as plasticity and hygroscopicity. The stability of linear polyelectrolytes is not ideal in long-standing high-humidity environments for breath monitoring.

All mentioned material (humidity-sensitive materials or functional materials)-based sensors involve substrate fabrication (for instance, interdigitated electrode printing [24,25]) and material transfer (for instance, deposition [17] or solidification [25–27]). In these procedures, maintaining the repeatability and consistency of sensing properties is a great challenge. These procedures will also reduce the mechanical strength and compactness of the sensor structure. Material transfer is laborious and time consuming, which reduces the practicability of sensors. Differences among the fabrication procedures could result in some sensing performance variations. In addition, materials might gradually spall off in long-term service. Therefore, breath monitoring based on a sensor with intrinsic fast-response humidity sensitivity and a compact structure is significant.

Herein, an ultrafast-response and compact fiber-optic humidity sensor was proposed and characterized using an eccentric fiber Bragg grating (EFBG) with an ultrawide cladding mode resonance range. Specifically, the EFBG was not combined with any humidity-sensitive material. Taking advantage of the highly refractive-index (RI)-sensitive last guided cladding mode, the EFBG could directly serve as a humidity-sensitive component. The EFBG was inscribed in a single-mode silica fiber, which was physically and chemically stable in a long-term high-humidity atmosphere. Humidity-induced RI changes in air can influence the interface evanescent field of guided cladding modes. Then, the guided cladding modes will rapidly respond to that RI change (including responses of wavelength and intensity). Consequently, an ultrafast response/recovery time (approximately 0.1 s) was obtained based on the EFBG humidity sensor. Furthermore, the core mode of the EFBG was quite stable for sensing humidity change and could be a great calibration for temperature perturbation and layout stability detection. The EFBG was utilized for real-time breath monitoring and could detect different breathing patterns. The EFBG shows excellent responsiveness, flexibility, robustness and repeatability and has promising potential for breath monitoring applications.

2. Methods of device fabrication

Fig. 1 shows the schematic of the EFBG. Generally, a normal fiber Bragg grating (FBG) involves a core mode and a comb with slight cladding modes that is induced by coupling between the forward-propagating core mode and backward-propagating modes along the

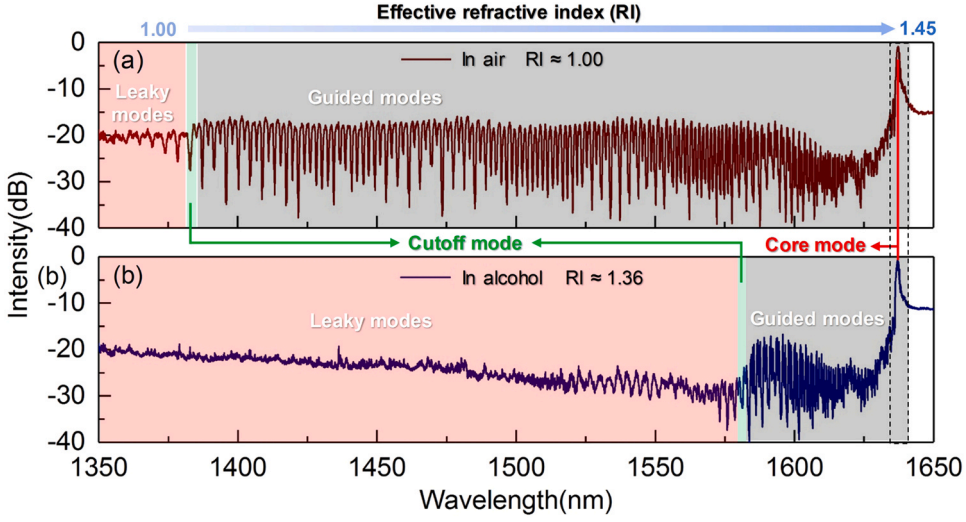

Fig. 3. (a) Original spectrum of the EFBG in air; (b) evolved spectrum of the EFBG in alcohol. Each mode type is covered by corresponding color patch in the spectrum.

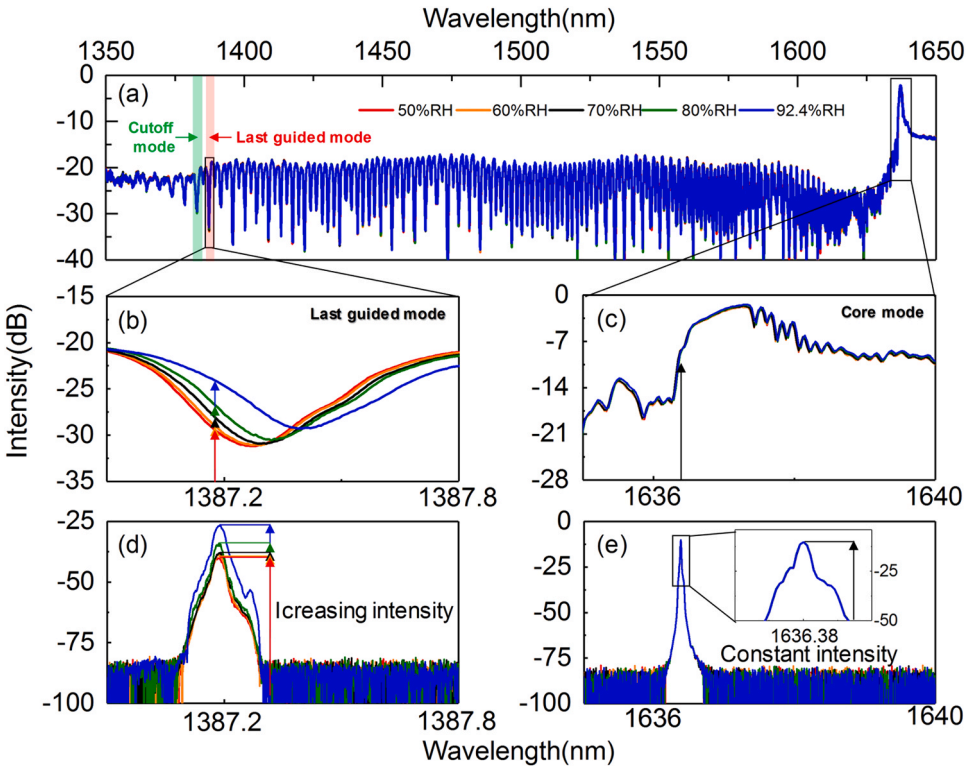

Fig. 4. Spectral responses of the EFBG versus different humidities: (a) whole spectrum (300 nm); (b) last guided mode; (c) core mode. Intensity responses of the single wavelength laser reflected by the EFBG: (d) last guided mode; (e) core mode.

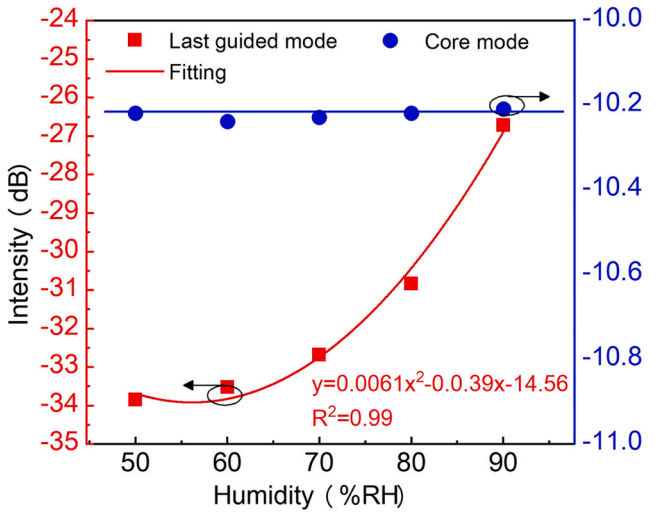

Fig. 5. Intensity responses of the EFBG versus different humidity (red symbol: last guided mode; blue symbol: core mode).

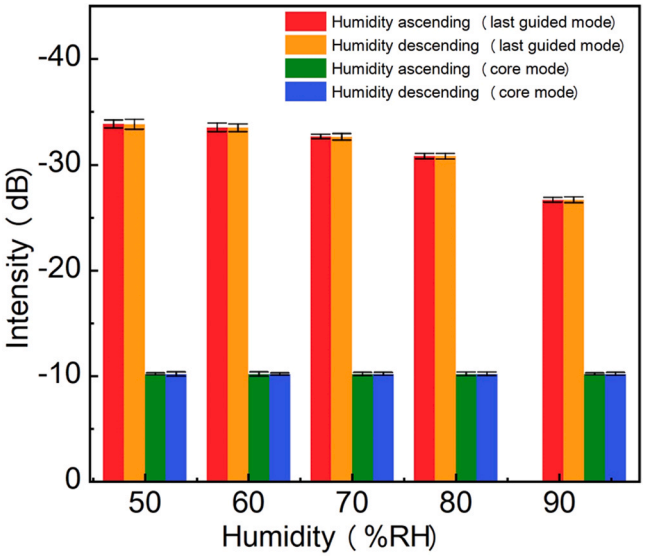

Fig. 6. Hysteresistestof the RH response (intensity responses of the single wavelength laser reflected by the EFBG).

cladding in the spectrum. The coupling strength is related to the position of the modulated RI that is induced in the optical fiber core by photo-inscription. The eccentric position of the modulated RI can magnify coupling extremely [35,36] The wavelength (λ) of the i-th cladding mode resonances is given by the following phase-matching conditions.

$$\lambda=(n_{eff,core}+n_{eff,clad,i})\Lambda/m \quad (1)$$

where $n_{eff,core}$ and $n_{eff,clad,i}$ are the effective RIs of the core mode and i-th cladding mode, respectively. Λ is the Bragg grating period along the fiber axis, and m is the order of grating. From Eq. (1), the ambient RI can influence the effective RI of the cladding modes, and further result in the resonant wavelength. This provides a mechanism to sense ambient RI.

The investigated EFBG was inscribed in a standard single-mode fiber (Corning SMF-28e) with a core diameter of approximately 9 μm using the point-by-point technique and a femtosecond laser (Spectra-Physics, Solstice, with a pulse width of 100 fs, a central wavelength of 800 nm, and a repetition rate of 1 kHz). The fiber was held on a three-dimensional (3D) translation stage (Newport Corp., XMS50 and GTS30V) for precise alignment and displacement. To inscribe the grating, the laser beam was focused in the fiber core by a 50 × oil-immersion microscope objective with a numerical aperture value of 1.25.

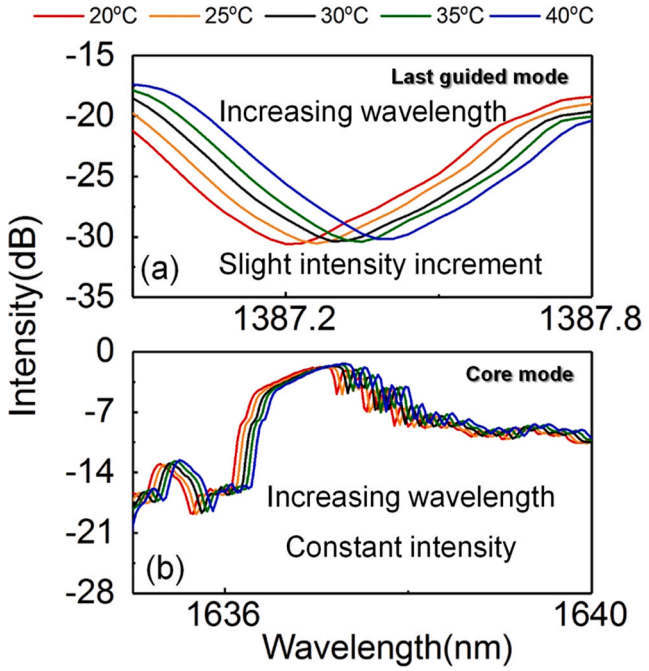

Fig. 7. Spectral responses of the EFBG versus different temperature: (a) last guided mode; (b) core mode.

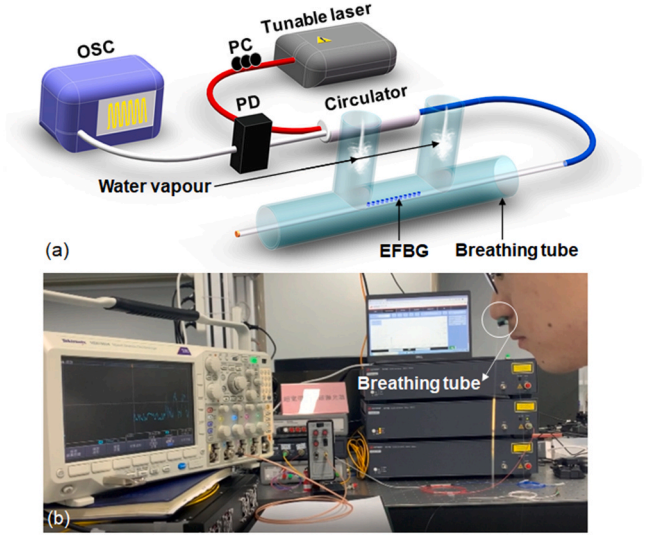

Fig. 8. (a) Experimental setup for breath monitoring; (b) photograph of a volunteer performing breathing trials.

The grating period was set to 1130 nm. Specifically, the focused laser beam was not centered in the fiber core but off-centered to magnify cladding mode coupling. During inscription, a series of periodic off-center RI modifications could be achieved inside the fiber core when the fiber was moved in relation to the focused laser beam, as shown in Fig. 2(a) and (b). Generally, EFBG devices are observed in the transmission spectrum [35], which requires two end connections. This is not convenient for subsequent measurement and packaging. Therefore, a gold film was coated on one end of the fiber (over 100 nm) by magnetron sputtering to reflect more than 90% broadband light, as shown in Fig. 2(c). Transmission was transformed to reflection. The gold film was used as a mirror and would not contribute to the sensing performance, the detailed comparison of different spectra is illustrated in Fig. S1 of Supplementary material. The fiber was not deformed or damaged but

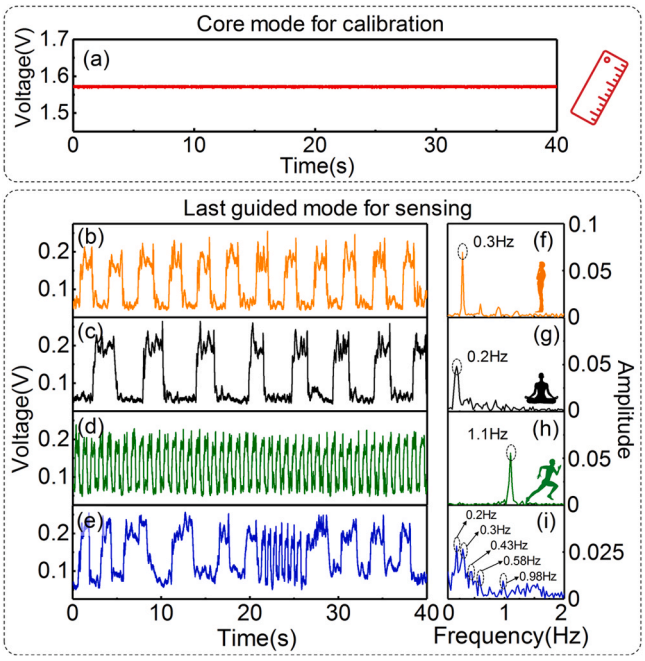

Fig. 9. (a) The real-time response of core mode. The responses of last guided mode to different breathing patterns: (b) normal; (c) slow; (d) fast; (e) random; and their corresponding FFT results: (f) normal; (g) slow; (h) fast; (i) random.

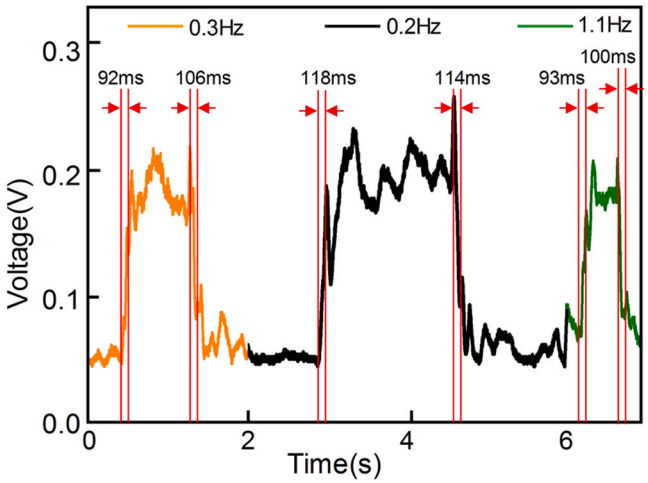

Fig. 10. Response and recovery times of the sensor versus different breathing.

was partly RI-modified in the core. In contrast to the structures of classic fiber humidity sensors, there was no restructuring, such as polishing [33], tapering [26,37] or splicing [34]. Some of optical fiber interferometers are relatively high-sensitive devices, while they are sensitive to many environmental parameters. They are not stable for breath motoring because humidity, temperature, airflow induced vibration can result in interferometric phase variation. Importantly, the fiber lateral surface was not combined with any sensitized materials, as the scanning electron micrograph shown in Fig. 2(d). The EFBG was very compact and easy to fabricate. Thus, the robustness, chemical stability, flexibility and nontoxicity of the optical fiber material (silica) were preserved. The EFBG can endure long-standing high-humidity atmospheres. Therefore, the EFBG is well suited for monitoring patients' breath status in terms of material properties.

Table 1
Comparison of humidity sensing performance on breath monitoring with reported works.

sensor	sensitized material type	response time/s	recovery time/s	self-compensation	Ref.
polyethylene naphthalate substrate with GO	2D material	0.03	0.03	N/A	[15]
P-doped silicon substrate with graphene	2D material	0.6	0.4	N/A	[16]
tilted optical fiber grating with GO	2D material	0.042	0.115	N/A	[17]
P-type silicon substrate with silicon nanowire	nanowire	–	–	N/A	[18]
plastic substrate with TiO_2 nanowires	nanowire	2.14	14.86	N/A	[23]
micro fiber knot resonator with gelatin	polymer	0.084	0.029	N/A	[26]
ceramic substrate with polyelectrolytes	polymer	0.29	0.47	N/A	[27]
multimode fiber with Au nanomembrane	metal	0.156	0.277	N/A	[32]
etched optical fiber with MoS_2	sulfide	0.066	2.395	N/A	[34]
EFBG (this work)	**not required**	**0.092**	**0.1**	**available**	/

3. Evaluation of refractive index response

Fig. 3(a) shows the resonant mode reflection of the EFBG in air (RI~1.00). The resonance located at the longest wavelength corresponds to the guided core mode, which is confined in the core (total reflection condition [38]). It remains stable when the ambient RI is changed. Here, the EFBG present a similar spectrum to tilted fiber Bragg grating (TFBG) [39,40], while the wavelength range of TFBG is dependent on titled angle. And the cladding modes comb of the TFBG is limited and discontinuous. In contrast, The EFBG has better spectral characteristics. Each cladding resonance mode has a one-to-one relative effective RI value according to Eq. (1), which can be modified by the ambient medium (including the wavelength and intensity). Cladding modes can be divided into three groups: the guided mode, cutoff mode and leaky mode. The guided modes are the cladding modes that have higher effective RI values than the ambient medium RI. The leaky modes are the cladding modes that have a lower effective RI value than the ambient medium RI. The cutoff mode is the boundary between guided modes and leaky modes. We can observe the cutoff cladding mode of the air medium in the reflection. When immersing the EFBG in alcohol (RI~1.36), partial guided modes will be suppressed or eliminated as the RI increases and is transformed to leaky modes. The intensities of guided modes will maintain their original spectral character because they satisfy propagation conditions [38]. However, the intensity of the transformed modes is weakened or even eliminated relative to their original state, as shown in Fig. 3(b). Importantly, the last guided mode next to the cutoff mode will be gradually transformed to a cutoff mode if the ambient RI is further increased. The evanescent field of the last guided mode is the most perturbed by the ambient RI; thus, it offers the maximum RI sensitivity [39,40].

4. Results and discussion

4.1. Humidity measurement

Humidity refers to the water vapor concentration in air, which can modify the effective RI of air to a certain extent. The last guided cladding mode that has an RI approximately equal to that of air can perceive RI modification because the air medium can rapidly affect the evanescent field of the last guided mode. To measure the humidity response, the EFBG was sealed in a homemade temperature and humidity chamber. The ambient temperature was set to 32 °C because the airflow temperature exhaled by humans is approximately 32 °C. The RH was stepwise increased from 50% to 92.4%RH, and each step was held for 30 mins to attain humidity stability. Here, the RI change induced by low water vapor concentration is undetectable for the evanescent field of the cladding mode, so the proposed sensor is insensitive in very low humidity atmosphere. It is a common problem for most breath monitoring methods based on humidity sensors [15,26], the effective operation range are generally from 40% to 90%RH.

Light from a broadband source (YSL SCseries) was launched into the EFBG through a polarizer, a polarization controller (PC) and a circulator. The input polarization state was adjusted to p-state. The reflection was recorded by an optical spectrum analyzer (OSA, AQ6317C, Yokogawa). The full spectrum responses of the EFBG to RH are shown in Fig. 4(a), and the local magnified spectra of the last guided mode and core mode are shown in Fig. 4(b) and (c). Clearly, as humidity increases, the last guided mode is affected by the water vapor concentration, but the core mode is unaffected. The last guided mode presents intensity fluctuation and wavelength shift because of the water vapor-induced RI increase. To characterize humidity responses more directly, the broadband source was replaced by a tunable laser (N7776C and N7778c, Keysight), and the wavelength of the laser was successively fixed at the edges of the last guided mode (1387.11 nm) and core mode (1636.38 nm), as shown by the arrow position in Fig. 4(b). The fluctuations of wavelength and intensity can be unified into the reflection intensity of the laser. Fig. 4(d) and (e) presents the laser reflection responses of the last guided mode and core mode to humidity, respectively. We plot the peak intensity amplitude of the laser reflection of the cladding mode and core versus different humidity, see Fig. 5. The response of cladding mode is not linear but quadratic fitting, and reflection of the core mode is quite stable. The core mode is insensitive to the humidity, contributing the potential system power monitoring based on the core mode intensity. The system power fluctuation can influence the humidity response of the last guided mode, which can be referred out by the core mode response. Thus, the core mode can be used as a power and wavelength reference. The hysteresis response of the EFBG was also measured by ascending and descending processes. As the results show in Fig. 6, the intensity amplitude of the last guided mode and core mode show consistent humidity responses during the processes of the humidity ascending and ascending, demonstrating the perfect repeatability of the EFBG.

4.2. Temperature measurement

Temperature cross-sensitivity is the drawback of most optical devices. Here, the temperature response of the EFBG was also experimentally investigated. The temperature was increased from 20 °C to 40 °C with a step of 5 °C. Ambient temperature can cause thermo-optic coefficient variations in fiber materials [41]. As a result, both the last guided mode and core mode present redshifts in wavelength with increasing temperature; see the experimental results shown in Fig. 7(a) and (b). The last guided mode presents a slight intensity increase that is negligible compared to the humidity-induced intensity change. Notably, the core mode presents redshifts in wavelength but not obvious intensity fluctuations. In addition, the core mode is insensitive to humidity, as discussed in last section. Therefore, during humidity monitoring, the temperature effect on the last guided mode can be calibrated by the response of the core mode. The wavelength self-compensation of the EFBG against different temperatures is available.

4.3. Breath monitoring

Humidity variation induced by breathing is generated in a short time

and usually lasts 3–5 s, and the response and recovery times are significant indicators of breath monitoring. Based on a measurement setup similar to the humidity test setup, a photodetector (PD) was used to convert the light intensity into electric signal. After passing through the circulator, the reflected light from the EFBG was monitored by an oscilloscope (Tektronix, MDO3000), as shown in Fig. 8(a). The EFBG was enclosed in a breathing tube to contact inhaled and exhaled air, illustrated in Fig. S2 of supplementary material. Also, attributing the micro size and excellent flexibility, the proposed sensor can be imbedded in other respiratory equipment, such as breathing tube, oxygen mask, and even be attached below the nose. The breathing tube was inserted the nasal cavity of the volunteer, as shown in Fig. 8(b). Again, the wavelength of the laser was successively fixed at the edges of the last guided mode (1387.11 nm) and core mode (1636.38 nm) to verify the response of these two modes to breath.

Four breath groups were validated, corresponding to normal breathing, deep breathing, fast breathing and random breathing. The response of the core mode to breath was measured first, as displayed in Fig. 9(a). The core mode was very stable during four measurements. The temperature in the breathing tube was maintained at approximately 30 °C. The response of the core mode confirmed that the temperature inside the breathing tube was relatively constant. Therefore, the temperature will not result in a significant effect on the measurement. Subsequently, the last guided mode was used to track breath activity (a demonstration video is available in the media materials), and breath was distinguished by the output high-level signal. The results detected were very consistent with actual breath. Normally, breath is steady and regular (see Fig. 9(b)). Under sleep and meditation conditions, breath will slow down (see Fig. 9(c)). To take in more oxygen during exercise, breath becomes rapid (see Fig. 9(d)). The breathing frequencies can be determined by obtaining fast Fourier transforms (FFT) (see Fig. 9(f)–(i)). For the last measurement of random breathing (Fig. 9(e) and (i)), five different frequencies are extracted from the result in the time domain. A demonstration video of monitoring human breath is presented in Video 1. Therefore, the proposed sensor can achieve high resolution for breath monitoring.

Supplementary material related to this article can be found online at doi:10.1016/j.snb.2021.130794.

From the results of the last guided mode (Fig. 9(b)-(e)), the high level is not flat but fluctuant, especially for low-frequency breath. Because optical fibers are not hydrophilic, they cannot absorb water molecules. The dispersed water molecules circled around the fiber with exhaled airflow and were not well distributed. Inevitably, human breathing can induce the variational airflow. The humidity of such airflow is not isotropous. However, the airflow induced vibration is not significant, as the results shown in Fig. 9(a), the response of core mode is unchanging. The grating period of EFBG and the elastic-optic coefficient of fiber material are negligible. Moreover, the frequency of that vibration induced by breath or speaking is much higher that breathing rate. The dominating voltage fluctuations of the results in Fig. 8 are contributed to breathing induced humidity change. This is a common phenomenon for breath monitoring in previous literature because the absorption capacity of hydrophilic material is also not always constant. It can be improved by steady-flow intake passage and signal filtering. However, monitoring is not significantly influenced by this matter, as presented in the above experimental results.

The corresponding response and recovery times of the four breathing frequencies are illustrated in Fig. 10. The response and recovery times are approximately 100 ms (at least 92 ms, at most 118 ms). In contrast, the response and recovery times of sensors in the literature are subject to breathing frequency because hydrophilic materials will absorb more water molecules and need a longer time to desorb water molecules at low frequencies. Thus, the residual water molecules in the materials of the last breath will affect the next one. Evidently, the proposed sensor addresses this problem. Moreover, with great robustness and chemical inertness, the sensor maintains very high performance for several weeks, indicating its excellent repeatability and long-term stability. The entire demonstration system can be replaced by several miniaturized electronic modules, and the real-time breath state can be outputted by a mobile phone app, as the integration module of sensing system shown in Fig. S3 of Supplementary material and demonstrated in Video 2. All modules are mature and cost-effective photoelectric or electronic components. We can match each mode resonance wavelength with corresponding LED. The wavelength of LED module can easily switch back and forth between the core mode wavelength and the last guided mode wavelength. And the size can be further reduced with the smaller modules and the simplified circuit board. The volume of sensing system and monitoring method are appropriate for wearable devices.

Supplementary material related to this article can be found online at doi:10.1016/j.snb.2021.130794.

Table 1 shows the reported humidity sensors developed for breath monitoring. Combining humidity-sensitive materials is the most common method, and graphene oxide (GO), nanophase silicon, supramolecular materials and hydrophilic polymers are good candidates. However, the sensing performance is subject to a combination effect between the sensitive material and substrate electrode. Achieving durable and reproducible sensors is challenging. The proposed sensor provides a new solution to breath monitoring, and it takes full advantage of its inherent sensing capability and avoids material combination. It still exhibits response and recovery times that are roughly equivalent to those of reported humidity sensors. Furthermore, based on the core mode response, it offers unique self-compensation capability for temperature and system power.

5. Conclusion

A novel all fiber-optic humidity sensor without any hydrophilic material combination, was proposed and experimentally demonstrated, presenting excellent performance for human breath monitoring. The sensing mechanism is based on the reaction between the evanescent field of the cladding mode and RI variation induced by exhaled water vapor. It eliminates the limitation of hydrophilic materials but offers fast response time (92 ms) and recovery time (100 ms). The proposed sensor demonstrated an excellent capability for breath-pattern sensing. The sensor is very compact, flexible, robust and stable. Moreover, it provides self-compensation capability for the system power and the temperature fluctuation. We believe that it is a promising candidate component for wearable devices and healthcare equipment.

CRediT authorship contribution statement

In this work, Weijia Bao, Fengyi Chen and Shen Liu jointly conceptualized and fabricated the devices, built the experimental setup. Weijia Bao and Huailei Lai carried out the experiments. Shen Liu and Yiping Wang provided help for the experiment. Weijia Bao wrote the original draft. Fengyi Chen and Huailei Lai helped to analyse the data. Shen Liu edited the manuscript. Yiping Wang helped to edit the manuscript.

Declaration of Competing Interest

The authors declare that they have no known competing financial interests or personal relationships that could have appeared to influence the work reported in this paper.

Acknowledgements

This work was supported by National Natural Science Foundation of China (NSFC) (61905160, 61905165, 61905164, 61905162); China National Postdoctoral Program for Innovative Talents (BX20190217); China Postdoctoral Science Foundation (2019M663044); Natural Science Foundation of Guangdong Province (2018KQNCX219); Science, Technology and Innovation Commission of Shenzhen Municipality (JCYJ20170818093743767).

Appendix A. Supporting information

Supplementary data associated with this article can be found in the online version at doi:10.1016/j.snb.2021.130794.

References

[1] T.Q. Trung, N.-E. Lee, Flexible and stretchable physical sensor integrated platforms for wearable human-activity monitoring and personal healthcare, Adv. Mater. 28 (2016) 4338–4372.
[2] N.D. Price, A.T. Magis, J.C. Earls, G. Glusman, R. Levy, C. Lausted, D.T. McDonald, U. Kusebauch, C.L. Moss, Y. Zhou, A wellness study of 108 individuals using personal, dense, dynamic data clouds, Nat. Biotechnol. 35 (2017) 747–756.
[3] A.T. Güntner, S. Abegg, K. Königstein, P.A. Gerber, A. Schmidt-Trucksäss, A. E. Pratsinis, Breath sensors for health monitoring, ACS Sens. 4 (2019) 268–280.
[4] P. Grossman, Breath, stress, and cardiovascular function, Psycho-Physiology 20 (1983) 284–300.
[5] L. Bernardi, C. Porta, A. Gabutti, L. Spicuzza, P. Sleight, Modula-tory effects of breath, Auton. Neurosci. 90 (2001) 47–56.
[6] Z. Fisar, J. Hroudová, H. Hansíková, J. Spáčilová, P. Lelková, L. Wenchich, R. Jirák, M. Zvěřová, J. Zeman, P. Martásek, J. Rab-och, Mitochondrial breath in the platelets of patients with Alz-heimer's disease, Curr. Alzheimer Res. 13 (2016) 930–941.
[7] J.A. Benjamin, K.E. Lewis, Sleep-disordered breathing and cardio-vascular disease, Postgrad. Med. J. 84 (2008) 15–22.
[8] F. Snyder, J.A. Hobson, D.F. Morrison, F. Goldfrank, Changes in breath, heart rate, and systolic blood pressure in human sleep, J. Appl. Physiol. 19 (1964) 417–422.
[9] A.M. Baig, Computing the effects of SARS-CoV-2 on breath regula-tory mechanisms in COVID-19, ACS Chem. Neurosci. 11 (2020) 2416–2421.
[10] M. Li, H. Li, W. Zhong, Q. Zhao, D. Wang, Stretchable conduc-tive polypyrrole/polyurethane (PPy/PU) strain sensor with netlike microcracks for human breath detection, ACS Appl. Mater. Inter-faces 6 (2014) 1313–1319.
[11] L.Q. Tao, K.N. Zhang, H. Tian, Y. Liu, D.Y. Wang, Y.Q. Chen, Y. Yang, T.-L. Ren, Graphene-paper pressure sensor for de-tecting human motions, ACS Nano 11 (2017) 8790–8795.
[12] F. Liao, Z. Zhu, Z. Yan, G. Yao, Z. Huang, M. Gao, T. Pan, Y. Zhang, Q. Li, X. Feng, Y. Lin, Ultrafast response flexible breath sensor based on vanadium dioxide, J. Breath. Res. 11 (2017), 036002.
[13] P. Jakkaew, T. Onoye, Non-contact respiration monitoring and body movements detection for sleep using thermal imaging, Sensors 20 (2020) 6307.
[14] S. Kano, K. Kim, M. Fujii, Fast-response and flexible nanocrystal-based humidity sensor for monitoring human breath and water evapo-ration on skin, ACS Sens. 2 (2017) 828–833.
[15] S. Borini, R. White, D. Wei, M. Astley, S. Haque, E. Spigone, N. Harris, J. Kivioja, T. Ryhänen, Ultrafast graphene oxide humidity sensors, ACS Nano 7 (2013) 11166–11173.
[16] A.D. Smith, K. Elgammal, F. Niklaus, A. Delin, A.C. Fischer, S. Vaziri, F. Forsberg, M. Råsander, H. Hugosson, L. Bergqvist, S. Schröder, S. Kataria, M. Östling, M. C. Lemme, Resistive graphene humidity sensors with rapid and direct electrical readout, Nanoscale 7 (2015) 19099–19109.
[17] B. Jiang, Z. Bi, Z. Hao, Q.C. Yuan, D.Y. Feng, K.M. Zhou, L. Zhang, X.T. Gan, J. L. Zhao, Graphene oxide-deposited tilted fiber grating for ultrafast humidity sensing and human breath monitoring, Sens. Actuators B-Chem. 293 (2019) 336–341.
[18] U. Mogera, A.A. Sagade, S.J. George, G.U. Kulkarni, Ultrafast response humidity sensor using supramolecular nanofibre and its application in monitoring breath humidity and flow, Sci. Rep. 4 (2014) 1–9.
[19] N. Shehada, J.C. Cancilla, J.S. Torrecilla, E.S. Pariente, G. Brön-strup, S. Christiansen, D.W. Johnson, M. Leja, M.P.A. Davies, O. Liran, N. Peled, H. Haick, Silicon nanowire sensors enable diagnosis of patients via exhaled breath, ACS Nano 10 (2016) 7047–7057.
[20] N. Shehada, G. Brönstrup, K. Funka, S. Christiansen, M. Leja, H. Haick, Ultrasensitive silicon nanowire for real-world gas sensing: noninvasive diagnosis of cancer from breath volatolome, Nano Lett. 15 (2015) 1288–1295.
[21] T. Saidi, D. Palmowski, S. Babicz-Kiewlicz, T.G. Welearegayd, N.E. Barib, R. Lonescu, J. Smulko, B. Bouchikhi, Exhaled breath gas sensing using pristine and functionalized WO3 nanowire sensors enhanced by UV-light irradiation, Sens. Actuat. B-Chem. 273 (2018) 1719–1729.
[22] L.F. Song, K.P. Dou, R.R. Wang, P. Leng, L.Q. Luo, Y. Xi, C.C. Kaun, N. Han, F. Y. Wang, Y.F. Chen, Sr-doped cubic In2O3/Rhombohedral In2O3 homojunction nanowires for highly sensi-tive and selective breath ethanol sensing: experiment and DFT simu-lation studies, ACS Appl. Mater. Interfaces 12 (2019) 1270–1279.
[23] C.H. Wu, W.H. Wang, C.C. Hong, K.C. Hwang, A disposable breath sensing tube with on-tube single-nanowire sensor array for on-site detection of exhaled breath biomarkers, Lab Chip 16 (2016) 4395–4405.
[24] R. j Xie, Q.J. Du, B.H. Zou, Y.Y. Chen, K. Zhang, Y.H. Liu, J.Y. Liang, B. Zheng, S. Li, W.N. Zhang, J.S. Wu, F.W. Huo, Wearable leather-based electronics for breath monitoring, ACS Appl. Biol. Mater. 2 (2019) 1427–1431.
[25] J.B. Yu, H.G. Byun, M.S. So, J.S. Huh, Analysis of diabetic patient's breath with conducting polymer sensor array, Sens. Actuators B-Chem. 108 (2005) 305–308.
[26] Y.T. Yi, Y.X. Jiang, H.Y. Zhao, G. Brambilla, Y.X. Fan, P.F. Wang, High-performance ultrafast humidity sensor based on microknot resonator-assisted Mach–Zehnder for monitoring human breath, ACS Sens. 5 (2020) 3404–3410.
[27] J.X. Dai, H.G. Zhao, X.Z. Lin, S. Liu, Y.S. Liu, X.P. Liu, T. Fei, T. Zhang, Ultrafast response polyelectrolyte humidity sensor for breath monitoring, ACS Appl. Mater. Inter. 11 (2019) 6483–6490.
[28] C. Harito, L. Utari, B.R. Putra, B. Yuliarto, S. Purwanto, S.Z.J. Zaidi, D.V. Bavykin, F. Marken, F.C. Walsh, Review—the development of wearable polymer-based sensors: perspectives, J. Electrochem. Soc. 167 (2020), 037566.
[29] Y. Xiao, J. Lin, O. Boric-Lubecke, M. Lubecke, Frequency-tuning technique for remote detection of heartbeat and breath using low-power double-sideband transmission in the Ka-band, IEEE T. Microw. Theory 54 (2006) 2023–2032.
[30] W. Lee, S.H. Cho, Integrated all electrical pulse wave velocity and breath sensors using bio-impedance, IEEE J. Solid-State Circ. 50 (2015) 776–785.
[31] P. Sanchez, C.R. Zamarreno, C.R. Zamarreo, M. Hernaez, I.R. Matias, F.J. Arregui, Exhaled breath optical fiber sensor based on LMRs for breath monitoring, Sensors (2014) 1142–1145 (IEEE).
[32] B.B. Du, D.X. Yang, Y.L. Ruan, P.P. Jia, H. Ebendorff-Heidepriem, Compact plasmonic fiber tip for sensitive and fast humidity and human breath monitoring, Opt. Lett. 45 (2020) 985–988.
[33] D.Q. Li, H.H. Lu, W.T. Qiu, J.L. Dong, H.Y. Guan, W.G. Zhu, J.H. Yu, Y.H. Luo, J. Zhang, Z. Chen, Molybdenum disulfide nanosheets deposited on polished optical fiber for humidity sensing and human breath monitoring, Opt. Express 25 (2017) 28407–28416.
[34] B.B. Du, D.X. Yang, X.Y. She, Y. Yuan, D. Mao, Y.J. Jiang, F.F. Lu, MoS2-based all-fiber humidity sensor for monitoring human breath with fast response and recovery, Sens. Actuators B-Chem. 251 (2017) 180–184.
[35] J.U. Thomas, N. Jovanovic, R.G. Becker, G.D. Marshall, M.J. With-ford, A. Tünnermann, S. Nolte, M.J. Steel, Cladding mode coupling in highly localized fiber Bragg gratings: modal properties and transmission spectra, Opt. Express 19 (2011) 325–341.
[36] J.U. Thomas, N. Jovanovic, R.G. Krämer, G.D. Marshall, M.J. With-ford, A. Tünnermann, S. Nolte, M.J. Steel, Cladding mode coupling in highly localized fiber Bragg gratings II: complete vectori-al analysis, Opt. Express 20 (2012) 21434–21449.
[37] J.M. Corres, F.J. Arregui, I.R. Matías, Sensitivity optimization of tapered optical fiber humidity sensors by means of tuning the thick-ness of nanostructured sensitive coatings, Sens. Actuators B-Chem. 122 (2007) 442–449.
[38] R. Kashyap. Fiber Bragg Gratings, Academic press,, 2009.
[39] Chen, C.; Guo, T.; Laronche, A.; Albert, J. Radiation mode resonances of tilted fiber Bragg gratings for high index media measurement. 19th International Conference on Optical Fibre Sensors. International Society for Optics and Photonics, 2008, 7004, 700418.
[40] T. Guo, F. Liu, Y. Liu, N.K. Chen, B.O. Guan, J. Albert, In-situ detection of density alteration in non-physiological cells with polari-metric tilted fiber grating sensors, Biosens. Bioelectron. 55 (2014) 452–458.
[41] G.B. Hocker, Fiber-optic sensing of pressure and temperature, Appl. Opt. 18 (1979) 1445–1448.

Weijia Bao was born in Inner Mongolia, China, in 1991. Weijia Bao received the Ph.D. degree in optics at the School of Physics, Northwest University, Xi'an, China, in 2018. He is currently a postdoctoral fellow at Shenzhen University. His main research interests include optical fiber sensing, special fiber grating devices and femtosecond laser micromachining.

Fengyi Chen was born in Shaanxi, China, in 1994. He received the B.S.degree in opto-electronic information science technology and engineering from the Northwest University, Xi'an, China. in 2016. He is currently working toward the Ph.D. degree in Optics with Northwest University.

Huailei Lai was born in Guangdong, China, in 2001. He is currently an undergraduate student at Shenzhen University. His major is Technique and Instrumentation of Measurements.

Shen Liu was born in Henan, China, in 1986. He received the M.S. degree in circuit and system from the Chongqing University of Posts and Telecommunications in 2013, and the Ph.D. degree in optical engineering from Shenzhen University, Shenzhen, China, in 2017. From 2017–2018, he was with Aston University, Birmingham, U.K., as a Postdoctoral Fellow. Since 2018, he has been with Shenzhen University, as an Assistant Professor. He has authored or coauthored 11 patent applications and more than 30 journal and conference papers. His current research interests focus on optical fiber sensors, WGMs resonator, and cavity optomechanics.

Yiping Wang was born in Chongqing, China, in 1971. He received the B.Eng. degree in precision instrument engineering from the Xi'an Institute of Technology, China, in 1995 and the M.S. and Ph.D. degrees in optical engineering from Chongqing University, China, in 2000 and 2003, respectively. From 2003–2005, he was with Shanghai Jiao Tong University, China, as a Postdoctoral Fellow. From 2005–2007, he was with the Hong Kong Polytechnic University, as a Postdoctoral Fellow. From 2007–2009, he was with the Institute of Photonic Technology (IPHT), Jena, Germany, as a Humboldt Research Fellow. From 2009–2011, he was with the Optoelectronics Research Centre (ORC), University of Southampton, U.K., as a Marie Curie Fellow. Since 2012, he has been with Shenzhen University, Shenzhen, China, as a Distinguished Professor. He has authored or coauthored a book, 21 patent applications, and more than 240 journal and conference papers. His current research interests focus on optical fiber sensors, fiber gratings, and photonic crystal fibers. Prof. Wang is a Senior Member of the Optical Society of America and the Chinese Optical Society.